JOURNAL OF PROPULSION AND POWER
Vol. 20, No. 2, March–April 2004

Supersonic Flow Ignition by Plasma Torch and H_2/O_2 Torch

Kan Kobayashi,* Sadatake Tomioka,† and Tohru Mitani‡
Japan Aerospace Exploration Agency, Miyagi 981-1525, Japan

The effectiveness of an H_2/O_2 torch igniter, which injects H_2/O_2 combustion gas, and a plasma torch igniter in promoting ignition of an H_2/air mixture within a supersonic combustor was investigated analytically and experimentally. First, bulk temperature and bulk radical concentration in an O_2 plasma torch igniter were estimated by asymptotic analysis. Those in the H_2/O_2 torch igniter were also obtained by equilibrium calculation. Second, gas sampling was conducted to determine the concentration of igniter injectant and the equivalence ratio in the region of ignition, namely, the recirculation region at the base of a rearward-facing step. Then, ignition time of the mixture in the region was analytically estimated by using a two-step H_2/O_2 reaction mechanism and the results just-mentioned. The estimation showed that the ignition promotion effect of the plasma torch igniter was higher than that of the H_2/O_2 torch igniter at a given input energy. However, the H_2/O_2 torch igniter was also expected to sufficiently promote ignition because it was easy to increase the input energy by increasing the mass flow rate. Thus, an ignition experiment with the H_2/O_2 torch igniter was conducted in Mach 2.5 airflow. Comparison of the results with those of the plasma torch igniters showed that the H_2/O_2 torch igniter also had a sufficient ignition promotion effect as expected from analytical results.

Nomenclature

A	=	constant
B	=	constant
C	=	constant
c_d	=	discharge coefficient
c_p	=	specific heat at constant pressure
E	=	strength of electric field, or energy
h	=	step height on the side walls of the combustor
k	=	reaction rate constant
$\dot{m}$	=	mass flux, or mass flow rate
P	=	pressure
R	=	gas constant
r	=	radial distance (with bar for normalized value)
s	=	integral variable
T	=	temperature (with bar for normalized value)
T_{total}	=	total temperature of airflow
t	=	time
u	=	velocity
X	=	mole fraction
x	=	axial distance from the step
z	=	axial distance
α_D	=	degree of dissociation
β	=	Zeldovich number
$\Gamma(a, b)$	=	an incomplete gamma function of the second kind, $\int_b^\infty e^{-t} t^{a-1}\,\mathrm{d}t$
η_{th}	=	thermal efficiency
λ	=	thermal conductivity
ρ	=	density
σ	=	electric conductivity
ς	=	inner variable
ϕ	=	equivalence ratio

Subscripts

A	=	atom (radical)
A_2	=	molecule
ad	=	adiabatic
auto_ig	=	autoignition
b	=	bulk
comp	=	composite solution
D	=	dissociation
I	=	ionization
ig	=	ignition
igniter	=	igniter injectant
in	=	inner solution
m	=	maximum
mix	=	mixture of stoichiometric H_2/air and igniter injectant
out	=	outer solution
PJ	=	plasma torch igniter
stoich	=	stoichiometric H_2/air mixture
TI	=	H_2/O_2 torch igniter
w	=	wall
0	=	initial

Presented as Paper 2001-1763 AIAA/NAL-NASDA-ISAS 10th International Space Planes and Hypersonic Systems and Technologies Conference, Kyoto, Japan, 24 April 2001; received 7 April 2003; revision received 10 October 2003; accepted for publication 26 October 2003.

*Researcher, Dual-Mode Combustion Group, Ramjet Propulsion Center, Kakuda Space Propulsion Center, Kimigaya, Kakuda; kobakan@kakuda-splab.go.jp. Member AIAA.

†Senior Researcher, Dual-Mode Combustion Group, Ramjet Propulsion Center, Kakuda Space Propulsion Center, Kimigaya, Kakuda. Member AIAA.

‡Group Leader, Dual-Mode Combustion Group, Ramjet Propulsion Center, Kakuda Space Propulsion Center, Kimigaya, Kakuda. Member AIAA.

Introduction

IN a scramjet engine, it is difficult to attain ignition and flameholding because of high flow velocity and short residence time. Thus, an igniter should be installed on the engine. For the promotion of ignition, various plasma torch igniters have been studied for many years,[1–9] and their effectiveness in promoting ignition has been proved.

Although a plasma torch igniter sufficiently promotes ignition, it requires a heavy battery and erosive electrodes. To minimize the engine weight and stabilize the engine operation, it is better to adopt another igniter that does not use such a battery and electrodes. The specific characteristic of a plasma jet is to have ions. Because ignition is promoted by addition of radicals and heat, if the amount of radicals resulting from the recombination of ions is sufficient igniter gas should be ionized. Kobayashi et al.[10] showed that the amount of radicals from the recombination could be ignored because of the low concentration of ions under the uniform temperature condition with a bulk temperature. However, a plasma jet is confined to the

center of the axisymmetric jet by the so-called pinch effect, and thus the plasma jet has a radial temperature distribution. Therefore, the amount of ions and radicals should be estimated with the temperature distribution. If the obtained radical concentration of the plasma jet is comparable to that of H_2/O_2 combustion gas, for instance, a spark-initiated H_2/O_2 torch igniter is promising as another igniter.

The purpose of this study was to investigate and compare the promotion of ignition by a plasma torch igniter with the temperature distribution and that by the H_2/O_2 torch igniter analytically and experimentally. A rectangular combustor with a rearward-facing step and H_2 fuel injection ports downstream of the step was considered, and an igniter was installed upstream of the step. First, asymptotic analysis of a plasma jet was conducted to obtain the temperature distribution and estimate the bulk temperature and bulk degree of dissociation in the jet. Those of the H_2/O_2 torch igniter were estimated by assuming an equilibrium condition. Second, gas sampling was carried out to determine both the H_2 fuel and the igniter injectant concentrations at the base of the step, which was observed to be the region of ignition in the combustor.[3] Third, ignition time of perfectly stirred static mixture with igniters was evaluated by using a two-step H_2/O_2 reaction mechanism and results of the estimations and gas sampling just-mentioned. Finally, an ignition experiment using the H_2/O_2 torch igniter was conducted in Mach 2.5 airflow, and the effects of the H_2/O_2 torch igniter were compared with those of a plasma torch igniter.[4]

Combustor and Flowfield

A rectangular combustor with rearward-facing steps was adopted in this study. The combustor consisted of two side walls, a top wall, and a bottom wall. Figure 1 shows a schematic diagram of the two side walls of the combustor as well as of the coordinate systems used in the present study. Both side walls had a rearward-facing step with a height of 3.2 mm ($=h$) for flameholding. The entrance cross section was 147.3 mm in height and 32 mm ($=10h$) in width. One side wall had four H_2 fuel-injection ports, each with a diameter of 4 mm at $x=12.8$ mm ($=4h$), and the other one had no injection ports. Room-temperature H_2 fuel was vertically injected at sonic speed. An igniter was installed at $x=-20$ mm on the side wall with H_2 fuel injectors. Hot gas in the igniter was also injected vertically at sonic speed. There were six taps along the step, each with a diameter of 1 mm at $x=0.5$ mm, and six other taps were on the line of $y=16$ mm (not shown in the figure). The former taps were for gas sampling, and the latter ones were for wall-temperature measurement to investigate ignition location.

Mach number, total temperature, and total pressure of the airflow were 2.5, 800–2500 K, and 1.0 MPa, respectively. Total temperature of airflow was controlled by a vitiation air heater that generated high-temperature flow by lean burning of H_2. Therefore, generated airflow contained H_2O. For a total temperature of airflow of 800 K, for example, the mole fraction of H_2O was 0.067, and was 0.375 for 2500 K. The mole fraction of O_2 in the airflow was kept at 21% by the addition of O_2.

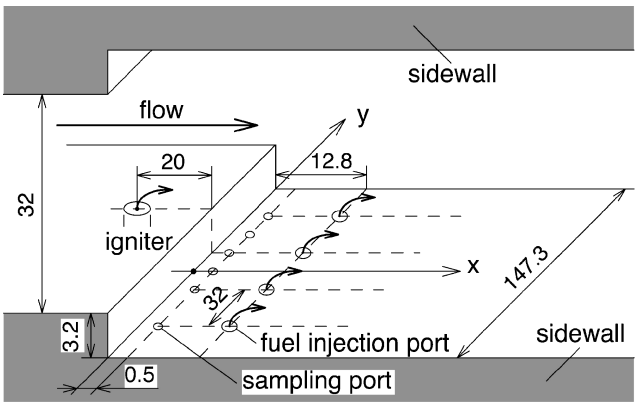

Fig. 1 Schematic diagram of a combustor for analysis and ignition experiment.

Analytical Discussion

Temperature and Radical Concentration in a Plasma Torch Igniter

Governing Equation

A plasma jet is considered to be an axisymmetric flow in a cooled cylinder. Figure 2 is a schematic diagram of an analytical model. Two kinds of temperature distribution, namely, distributed temperature and uniform temperature, are shown in the figure. The objective of the analysis is to quantitatively estimate bulk temperature and bulk radical concentration in the plasma jet with a distributed temperature. For comparisons, these bulk values with a uniform temperature are also estimated.

To simplify the governing equation, three assumptions are made: 1) the plasma jet is a steady flow, 2) pressure is constant at 0.1 MPa, and 3) heat conduction in the z direction is negligible. Then, the governing energy equation is expressed as

$$c_p\dot{m}\frac{\partial T}{\partial z}=\frac{1}{r}\frac{\partial}{\partial r}\left(r\lambda\frac{\partial T}{\partial r}\right)+E^2\sigma \tag{1}$$

Because the electric conductivity is proportional to an exponential function of temperature, it has a strong temperature dependency. A further assumption, 4) that the flow is fully developed, makes it possible to ignore the temperature distribution in the z direction. Finally, the governing equation to be solved is rewritten as

$$\frac{1}{r}\frac{\mathrm{d}}{\mathrm{d}r}\left(r\lambda\frac{\mathrm{d}T}{\mathrm{d}r}\right)+E^2\sigma_1\exp\left(-\frac{T_I}{2T}\right)=0 \tag{2}$$

where T_I is the characteristic ionization temperature. Equation (2) is the so-called Elenbaas–Heller equation,[11] which shows that the heat conduction term in the r direction and Joule's heating term balance out. The boundary conditions at the center of the plasma jet and at the wall are

$$T=T_m \quad \text{at} \quad r=0, \quad \text{and} \quad T=T_w \quad \text{at} \quad r=r_w \tag{3}$$

where T_m is the maximum temperature of the plasma jet and T_w is the gas temperature at the wall.

Previously, Sudano[12] solved the Elenbaas–Heller equation with constant transport coefficients and obtained the temperature distribution in the plasma jet. The difference between the former analysis and the present one is the way of treating Joule's heating term, which affects the temperature distribution. Although Joule's heating term was treated as a constant in the former analysis, it is treated as a function of temperature in the present analysis so as to accurately determine the temperature distribution. Therefore, the governing equation became a nonlinear equation with a strong temperature dependency, which is favorable for the asymptotic analysis.

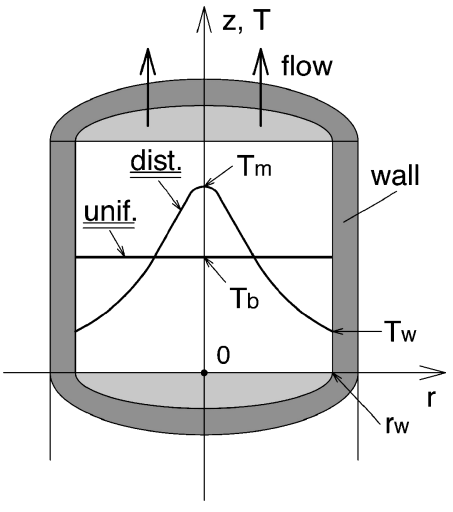

Fig. 2 Schematic diagram of a plasma jet for asymptotic analysis.

Nondimensionalization

Equations (2) and (3) are nondimensionalized by the radius r_w and the maximum temperature T_m as follows:

$$\frac{1}{\bar{r}}\frac{\mathrm{d}}{\mathrm{d}\bar{r}}\left(\bar{r}\frac{\mathrm{d}\bar{T}}{\mathrm{d}\bar{r}}\right)+A_1\exp\left\{\frac{\beta_I}{2}\left(1-\frac{1}{\bar{T}}\right)\right\}=0 \tag{4}$$

where

$$A_1=\frac{r_w^2E^2\sigma_1\exp(-\beta_I/2)}{T_m\lambda} \tag{5}$$

$$\bar{T}=1 \quad \text{at} \quad \bar{r}=0, \quad \text{and} \quad \bar{T}=\bar{T}_w \quad \text{at} \quad \bar{r}=1 \tag{6}$$

Here, variables with a bar represent normalized values only for temperature and radial distance, and β_I is an ionization Zeldovich number ($\equiv T_I/T_m$). Thermal conductivity is assumed to be constant for the sake of simplicity. Joule's heating term is modeled using an exponential function with respect to β_I and T. Because β_I is a large parameter around 10, Joule's heating term has a strong temperature dependency, which enables us to seek analytical asymptotic solutions.

Temperature Distribution

In the region in which the normalized temperature is much less than unity, Joule's heating term can be ignored because it is exponentially small. The temperature distribution in this region, an outer solution, is the solution of the heat-conduction equation

$$\bar{T}_{\mathrm{out}}=\bar{T}_w-B_1\,\ell_n(\bar{r}) \tag{7}$$

where B_1 is an integral constant to be determined by matching the outer solution with an inner solution obtained later. Note that the outer solution does not satisfy the inner boundary condition because $\bar{r}=0$ is a singular point on $\ell_n(\bar{r})$.

On the other hand, Joule's heating term cannot be ignored in the high-temperature region around the center of the plasma jet. The temperature distribution in this region, an inner solution, is the solution of the equation expressed by an inner variable ζ as follows:

$$\bar{T}_{\mathrm{in}}=1-(4/\beta_I)\,\ell_n\left(1+A_2\zeta^2\right) \tag{8}$$

where

$$\zeta=\exp\left(\frac{B_2\beta_I}{2}\right)r, \qquad A_2=\frac{A_1\beta_I\exp(-B_2\beta_I)}{16} \tag{9}$$

B_2 is also an integral constant. The inner solution satisfies only the inner boundary condition.

By matching the inner solution with the outer one, a composite solution is obtained as

$$\bar{T}_{\mathrm{comp}}=1-(4/\beta_I)\,\ell_n\left\{1+\exp([(1-\bar{T}_w)/4]\beta_I)\bar{r}^2\right\} \tag{10}$$

Radial temperature distribution in a plasma jet for $\bar{T}_w=0.1$ is shown in Fig. 3. The figure indicates that the solution is an asymptotic solution for large β_I. Because a larger β_I leads to a strong temperature dependency on Joule's heating, the temperature gradient around the center is greater for larger β_I. In other words, a larger β_I results in confinement of the heating to around the center of the plasma jet.

Bulk Temperature

From the temperature distribution in a plasma jet obtained from the asymptotic analysis, namely, Eq. (10), the bulk temperature can be estimated. The bulk value is defined as the so-called cup-mixing value. Thus, the bulk temperature of the plasma jet is written as

$$\bar{T}_b=\frac{2\pi\int_0^1\bar{T}\dot{m}\bar{r}\,\mathrm{d}\bar{r}}{2\pi\int_0^1\dot{m}\bar{r}\,\mathrm{d}\bar{r}} \tag{11}$$

Because the plasma jet is considered to be in a state of thermal choking, its mass flux is inversely proportional to the square root of the temperature. Therefore, the preceding equation is expressed and integrated as a function of temperature. As a result, the bulk temperature can be obtained as

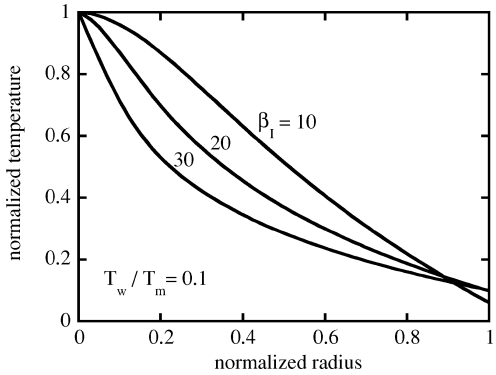

Fig. 3 Radial temperature distributions in a plasma jet for $\bar{T}_w=0.1$ and $\beta_I=10, 20, 30$.

$$\bar{T}_b=\frac{4}{\beta_I}\frac{\Gamma[3/2,(\beta_I/4)\bar{T}_w]-\Gamma(3/2,\beta_I/4)}{\Gamma[1/2,(\beta_I/4)\bar{T}_w]-\Gamma(1/2,\beta_I/4)} \tag{12}$$

Bulk Degree of Dissociation

The bulk degree of dissociation in the plasma jet is also expressed in the same form as in the case of the bulk temperature as

$$\alpha_{D,b}=\frac{2\pi\int_0^1\alpha_D\dot{m}\bar{r}\,\mathrm{d}\bar{r}}{2\pi\int_0^1\dot{m}\bar{r}\,\mathrm{d}\bar{r}} \tag{13}$$

The same procedure for obtaining the bulk temperature leads to the following solution as the bulk degree of dissociation, namely,

$$\alpha_{D,b}=\frac{1}{\sqrt{C_D}}\frac{\int_{(\beta_I/4)\bar{T}_w}^{\beta_I/4}s^{-\frac{1}{2}}\exp[-s-(\beta_I\beta_D/8)(1/s)]\,\mathrm{d}s}{\Gamma[1/2,(\beta_I/4)\bar{T}_w]-\Gamma(1/2,\beta_I/4)} \tag{14}$$

where $C_D=4P/P_D$ and β_D is a dissociation Zeldovich number ($\equiv T_D/T_m$). Here, P_D and T_D are dissociation characteristic pressure and temperature, respectively. The results show that these bulk values are functions of β_I and β_D. Because T_I and T_D are known for each feedstock, these bulk values are obtained at a given maximum temperature related to an input energy. Note that a thermal conductivity does not appear in the temperature distribution [Eq. (10)], the bulk temperature [Eq. (12)], and the bulk degree of dissociation [Eq. (14)]. When estimating T_m from the input energy, for instance, thermal conductivity is required.

Bulk Values and Input Energy

Input energy to a plasma torch igniter can be separated into two, namely, thermal energy and chemical energy. The former energy can be estimated from the temperature of the plasma jet. The latter energy, on the other hand, can be obtained from the radical concentration and its enthalpy of formation. Thus, molecules of the igniter injectant have only thermal energy, and radicals have both thermal energy and chemical energy. Both kinds of energy are estimated by using the obtained bulk values and the Joint Army-Navy-Air Force (JANAF) table.[13] The summation of these two kinds of energy is defined as input energy in the present analysis.

Figure 4 shows the bulk degree of dissociation and ionization of an O_2 plasma jet as a function of the input energy. The bulk degree of dissociation was obtained from Eq. (14). The degree of ionization was obtained by using β_I and $C_I=P/P_I$ instead of β_D and C_D in Eq. (14). Solid lines show the results for a distributed temperature in the plasma jet for $T_w=1000$ K, and broken lines show those for a uniform temperature. The condition of uniform temperature means that temperature in the whole area corresponds to the bulk

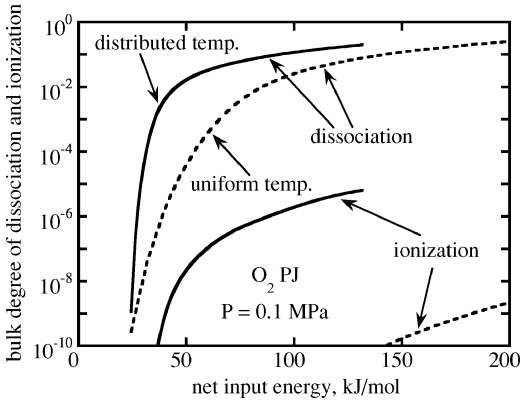

Fig. 4 Bulk degree of dissociation and ionization in an O_2 plasma torch igniter as a function of input energy for $P = 0.1$ MPa.

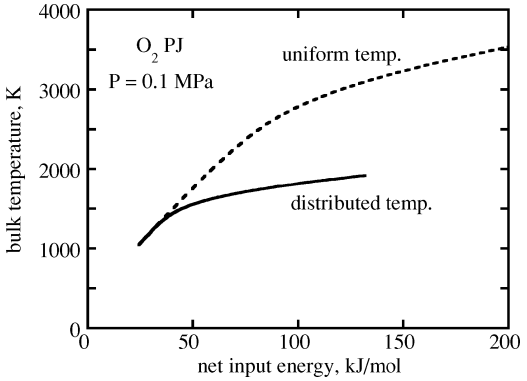

Fig. 5 Bulk temperature in an O_2 plasma torch igniter as a function of input energy for $P = 0.1$ MPa.

temperature. The figure indicates the amount of chemical energy absorbed as dissociation and ionization energy in the plasma jet.

Figure 4 also indicates that the temperature distribution causes a larger degree of dissociation and ionization than in the case of uniform temperature at a given input energy. In the case of $E_{\text{input}} = 120$ kJ/mol, for example, the distributed temperature leads to a three-fold increase in the degree of dissociation as compared with the case of uniform temperature. Because larger input energy leads to almost complete dissociation, the effect of temperature distribution on the degree of dissociation is smaller for larger input energy. The degree of ionization is much smaller than that of dissociation, even in the case of distributed temperature. Therefore, radicals resulting from the recombination of ions are negligible.

The relationship between the input energy and the bulk temperature of the O_2 plasma jet is presented in Fig. 5, which indicates the amount of absorbed thermal energy. Gas temperature at the wall was fixed at 1000 K for the case of distributed temperature. The figure shows that assuming a uniform temperature distribution results in a higher bulk temperature than that for distributed temperature at a given input energy. The reason for this is that the plasma jet with a distributed temperature has a greater degree of dissociation and hence a larger chemical energy than that with a uniform temperature, as shown in Fig. 4. In the case of $E_{\text{input}} = 120$ kJ/mol, for example, the bulk temperature for a uniform temperature is 3000 K, although that for a distributed temperature is 1900 K.

Because a temperature distribution in a plasma jet affects the bulk degree of dissociation and the bulk temperature as shown in Figs. 4 and 5, respectively, it cannot be ignored as mentioned before. Therefore, only the case with a distributed temperature will be considered in the following analysis for a plasma jet.

Temperature and Radical Concentration in an H_2/O_2 Torch Igniter

Although the plasma jet is confined to the center by the pinch effect, combustion gas in an H_2/O_2 torch igniter is uniformly generated. Therefore, the radial temperature distribution of the combustion gas jet can be ignored. Because the residence time of gas in H_2/O_2 torch igniter was found to be much longer than the reaction time of H_2/O_2 mixture under the experimental conditions shown later, equilibrium calculation was conducted to determine the bulk values in the H_2/O_2 torch igniter. LSENS[14] was used for the equilibrium calculation under the stoichiometric condition within the H_2/O_2 torch igniter for $P = 0.1$ MPa and $T_0 = 300$ K. Results showed that the equilibrium temperature was 3080 K and that the equilibrium radical mole fraction defined as $X_O + X_H + X_{OH}$ was 0.217. Thus, input energy to the H_2/O_2 torch igniter in this condition was 140 kJ/mol.

In the case of the O_2 plasma torch igniter with an input energy of 140 kJ/mol, on the other hand, Figs. 4 and 5 show that the bulk temperature and bulk degree of dissociation were 1910 K and 0.244, respectively. The bulk degree of dissociation of 0.244 corresponds to the radical mole fraction of 0.392 because of the relationship

$$X_A = \frac{2\alpha_{D,A2}}{1 + \alpha_{D,A2}} \tag{15}$$

Therefore, injectant from the H_2/O_2 torch igniter had a 60% higher temperature and a 45% lower radical mole fraction than the case of the O_2 plasma torch igniter for the input energy of 140 kJ/mol.

Injectant Concentration in the Region of Ignition

In the previous ignition experiment[3] using a rectangular combustor with a rearward-facing step, ignition first took place at the base of the step when the total temperature of airflow was increased. Therefore, the conditions of the mixture in the recirculation region were evaluated experimentally and used for calculating the ignition time.

Gas sampling through taps on the side wall was conducted at six locations along the base of the step, and sampled gas was analyzed by gas chromatography. The mixture for calculation of ignition time consists of vitiated air, H_2 fuel, and igniter injectant. Here, the igniter injectant consists of H_2O (and residual H_2 for fuel-rich condition). Because H_2O cannot be detected by gas chromatography, another gas except N_2, O_2, and H_2, which were contained in the main flow, should be applied as a simulated injectant. Therefore, He was injected as a simulated injectant in the present study. H_2 fuel was injected at a bulk equivalence ratio of 0.1–0.4, and He with room temperature was injected from a simulated igniter at 0.55 MPa. Total temperature of airflow was fixed at 1500 K. The measured mole fraction of He was transformed to a mass fraction. The mass fraction was assumed to be identical to that of the igniter injectant. Then, the estimated mass fraction of the igniter injectant was retransformed to a mole fraction. The effects of the assumption on the results of the gas sampling will be discussed later.

Figure 6 indicates the spanwise distribution of the local equivalence ratio at the base of the rearward-facing step. The experimental uncertainty was ± 0.05 in the equivalence ratio. A high equivalence ratio was observed upstream of the H_2 fuel-injection ports.

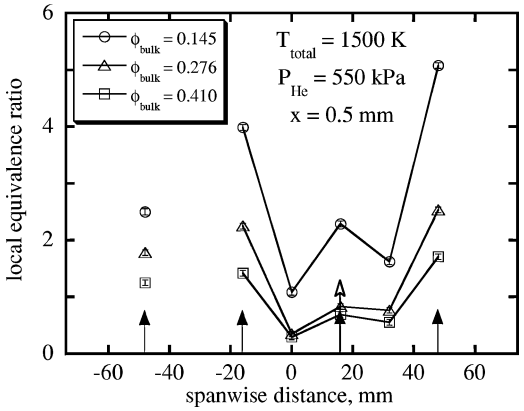

Fig. 6 Spanwise distributions of equivalence ratio at the base of a rearward-facing step for $T_{\text{total}} = 1500$ K and $P_{\text{He}} = 550$ kPa.

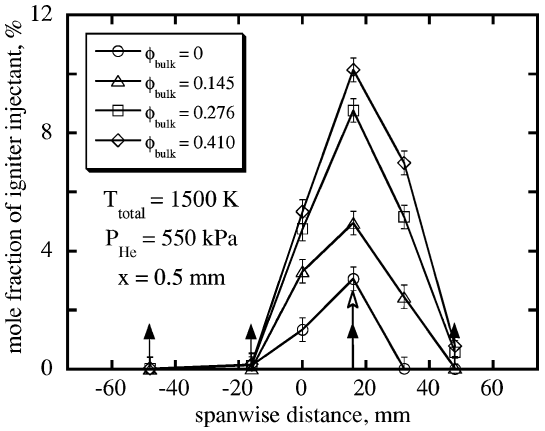

Fig. 7 Spanwise distributions of igniter injectant volume concentration at the base of a rearward-facing step for $T_{total} = 1500$ K and $P_{He} = 550$ kPa.

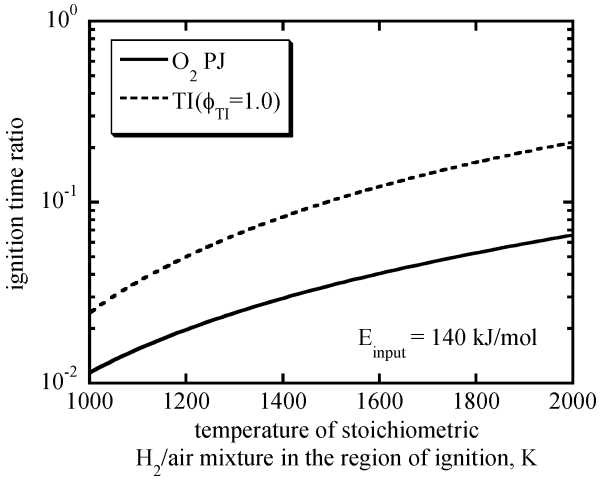

Fig. 8 Ignition time ratio with an O_2 plasma torch igniter and an H_2/O_2 torch igniter.

Therefore, the location with a lower equivalence ratio than that at $y = -16$ and -48 mm would be between these points, so that these data should not be joined directly. The local equivalence ratio decreased with an increase in the bulk equivalence ratio. The reason for this was that a higher bulk equivalence ratio resulted in a higher injection pressure and in a larger penetration of fuel into the airflow, leaving a small fraction of the fuel within the recirculation region. The local equivalence ratio downstream of the igniter was almost 1.0 for the bulk equivalence ratio of 0.4.

Spanwise distributions of the mole fraction of igniter injectant in the recirculation region are shown in Fig. 7. The experimental uncertainty was $\pm 0.4\%$ in the mole fraction. Solid and open arrows represent the locations of H_2 fuel injection and He injection, respectively. The mole fraction of the igniter injectant was found to be maximum downstream of the igniter. Furthermore, it increased with an increase in the bulk equivalence ratio because of the lesser fraction of fuel in the recirculation region. The maximum mole fraction of the igniter injectant was 10% for the bulk equivalence ratio of 0.4.

Ignition Time with Igniters

To estimate the ignition promotion effects by igniters analytically, ignition time of the mixture in the recirculation region is evaluated in this section by using the results already obtained. Perfectly stirred static mixture was adopted because of the low velocity at the base of the step. A two-step H_2/O_2 reaction mechanism[15] that consists of a chain-initiation reaction ($H_2 + O_2 \rightarrow OH + OH$: $R6$) and a chain-branching reaction ($H + O_2 \rightarrow OH + O$: $R1$) was adopted for the calculation. Time variation of the radical mole fraction is then written as

$$\frac{dX_{rad.}}{dt} = \frac{X_{rad.}}{t_1} + \frac{X_{H_2,0}}{t_6} \tag{16}$$

where $t_1 = (k_1[O_2]_0)^{-1}$ and $t_6 = (2k_6[O_2]_0)^{-1}$ are the characteristic reaction times of $R1$ and $R6$, respectively, and $[O_2]$ is a mole concentration of O_2. Note that O and OH are replaced with H by faster reactions than $R1$ in the case of multistep H_2/O_2 reaction mechanism. When considering the reactions of $H_2 + O \rightarrow H + OH$ ($R2$) and $H_2 + OH \rightarrow H + H_2O$ ($R3$), $k_2/k_1 \approx 4$ and $k_3/k_1 \approx 6$ are obtained for $T = 1500$ K, for instance. Therefore, the steady-state approximations of O and OH could be applied, and thus X_H corresponded to $X_{rad.}$ in the first term of the right-hand side of Eq. (16). Furthermore, concentrations of H_2 and O_2 were assumed to be constant because of their sufficient amounts. The characteristic reaction times are a function of reaction-rate constants[16] and temperature. When the two boundary conditions, $X_{rad.} = X_{rad.,0}$ at $t = 0$ and $X_{rad.} = X_{rad.,ig}$ at $t = t_{ig}$, are satisfied, the ignition time is expressed as follows:

$$t_{ig} = t_1 \ln \frac{1 + (X_{rad.,ig}/X_{H_2,0}) \cdot (t_6/t_1)}{1 + (X_{rad.,0}/X_{H_2,0}) \cdot (t_6/t_1)} \tag{17}$$

Here, the mixture was considered to ignite when the radical mole fraction reached 5%. Because the ignition time in the region of ignition was expressed as a function of the radical mole fraction and temperature in this way, it was possible to estimate the effects of the increase in temperature and radical mole fraction by the igniters.

For the calculation, the injectant concentration and equivalence ratio in the mixture must be given to determine the initial temperature and composition. Therefore, the injectant concentration and equivalence ratio were assumed to be 10% and 1.0, respectively. According to the experimental results shown in Figs. 6 and 7, this condition corresponds to that downstream of the igniter for a bulk equivalence ratio of 0.4.

Autoignition time is also a function of temperature, and so we normalized the ignition time with igniters by autoignition time to evaluate the effect of igniters on ignition promotion. Therefore, a smaller ignition time ratio indicates a greater ignition promotion effect. Figure 8 shows the ignition time ratio t_{ig}/t_{auto_ig}, with igniters for $E_{input} = 140$ kJ/mol. The solid line and the broken line represent the results of an O_2 plasma torch igniter and an H_2/O_2 torch igniter, respectively. Temperature of the mixture in the region of ignition T_{mix} was calculated as $T_{mix} = 0.9T_{stoich} + 0.1T_{igniter}$, where T_{stoich} and $T_{igniter}$ were temperatures of stoichiometric H_2/air mixture and igniter injectant, respectively. $T_{mix} = T_{stoich}$ was applied only for calculating autoignition time. Higher T_{stoich} leads to lower ignition promotion effects because the relative increment of temperature by igniters becomes smaller for a higher T_{stoich}. Note that the initial mole fraction of radicals $X_{rad.,0}$ was calculated by the same way for T_{mix}.

The ignition time ratio by the O_2 plasma torch igniter was less than that by the H_2/O_2 torch igniter at a given T_{stoich}. Therefore, a higher T_{stoich} is required for the H_2/O_2 torch igniter to obtain the same ignition time as that by the O_2 plasma torch igniter. For $T_{stoich} = 1000$ K, for instance, the ignition time ratios by the O_2 plasma torch igniter and the H_2/O_2 torch igniter were 0.011 and 0.024, respectively. As a result, $T_{stoich} = 1200$ K is required for the H_2/O_2 torch igniter to obtain the same ignition time as that by the O_2 plasma torch igniter. This shows that the ignition promotion effect of a plasma torch igniter is higher than that of the H_2/O_2 torch igniter at a given input energy.

As already mentioned, the mass fraction of He was assumed to be identical to that of the igniter injectant in the gas sampling. Thayer and Corlett[17] and Zamma et al.[18] investigated the relationship between mass fraction and kinds of gas. Thayer and Corlett showed that mass fraction was a function of RT ratio. Zamma et al., on the other hand, showed that it was a function of ρu ratio. Their empirical equations show that the mass fraction of the igniter injectant is reduced from that of He by 20–25%. Because the flowfields of their experiments are different from the present one, the value cannot be

applied directly. Furthermore, even if the mass fraction of the igniter injectant is assumed to be 25% smaller than that of He, the conclusion that the ignition promotion effect of a plasma torch igniter is greater than that of the H_2/O_2 torch igniter at a given input energy is not affected. Therefore, the assumption adopted in the present study was appropriate.

Here, we are interested in which more effectively promotes ignition, thermal effects or chemical effects. In other words, "Which is more effective for ignition promotion, to use energy for heating feedstock as thermal energy or to use it for producing radicals as chemical energy at a given input energy?" The ignition time in the analysis is expressed as a function of temperature and radical concentration. Therefore, it is possible to compare two kinds of ignition time, namely, one in which only the temperature rise by igniters is considered and the other in which only the increment of radical concentration by igniters is considered. When input energy is equally divided into two, namely, thermal energy = chemical energy, the just-mentioned comparison gives us the answer.

Figure 9 shows the relationship between total input energy and energy fraction in the O_2 plasma torch igniter with a temperature distribution. Thermal energy and chemical energy were obtained by the bulk temperature [Eq. (12) and Fig. 5] and the bulk degree of dissociation [Eq. (14) and Fig. 4], respectively. These bulk values were obtained by using temperature distribution [Eq. (10)] for O_2 plasma jet. An increment of input energy leads to an increment of the fraction of chemical energy and a decrement of the fraction of thermal energy. At a total input energy of 100 kJ/mol, thermal energy and chemical energy are almost identical. Therefore, calculation of ignition time at this input energy is necessary to determine which energy more effectively promotes ignition.

Figure 10 is the relationship between ignition time ratio and T_{stoich} at a total input energy of 100 kJ/mol. The solid line shows the result of ignition promotion by both radicals and heat. The broken lines, on the other hand, show that by radicals or heat. The ignition promotion effect by only radicals was greater than that by only heat. For $T_{\text{stoich}} = 1400$ K, for example, radical addition reduced the ignition time by 90%, whereas heat addition reduced it by only 40%. Therefore, if we can choose the use of input energy in this model it is better to use the energy for producing radicals.

The result obtained in Fig. 10 explains that in Fig. 8 as follows. The O_2 plasma torch igniter with a distributed temperature led to a three-fold increase in the fraction of chemical energy as compared with the case of the H_2/O_2 torch igniter with a uniform temperature for $E_{\text{input}} = 140$ kJ/mol. This is because the distributed temperature led to a larger degree of dissociation than the uniform temperature as shown in Fig. 4. As a result, the O_2 plasma torch igniter with a larger fraction of chemical energy, namely, with a more effective configuration for ignition, than the H_2/O_2 torch igniter showed a shorter ignition time at a given input energy. However, it is easy to increase the input energy to the H_2/O_2 torch igniter by increasing the flow rate as will be shown in the experiment. Therefore, sufficient promotion of ignition can be obtained not only by an O_2 plasma torch igniter but also by an H_2/O_2 torch igniter.

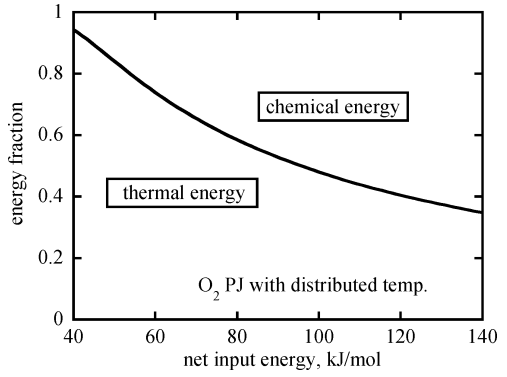

Fig. 9 Energy fraction within an O_2 plasma torch igniter with a distributed temperature.

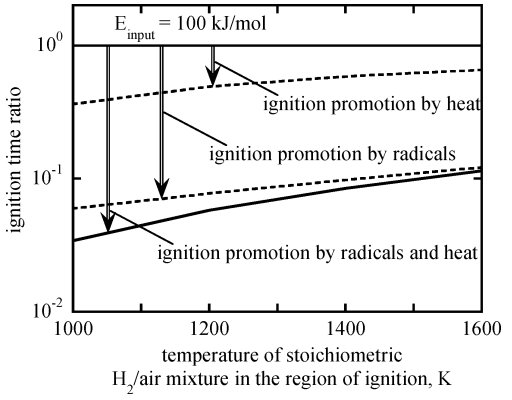

Fig. 10 Ignition time ratio with an O_2 plasma torch igniter with a distributed temperature.

Ignition Experiments with Igniters

Experimental Conditions

To verify the prediction that the H_2/O_2 torch igniter sufficiently promotes ignition, an ignition experiment was conducted at the Japan Aerospace Exploration Agency, Kakuda Space Propulsion Center. Airflow conditions and the combustor were explained in the Combustor and Flowfield section. Because the experimental apparatus was the same as that used in the previous experiments with a plasma torch igniter,[4] the ignition promotion effect of the H_2/O_2 torch igniter could be compared with that of the plasma torch igniter.

Figure 11 shows a schematic diagram of the H_2/O_2 torch igniter, which was installed at $x = -20$ mm. It had no active cooling system and was made of copper because of its high heat conductivity. The H_2/O_2 torch igniter was 150 mm in length. H_2 and O_2 were injected through calibrated orifices into a cylindrical combustion chamber with a diameter of 10 mm. Flow rates of H_2 and O_2 were determined based on the discharge coefficients of these orifices. The equivalence ratio in the H_2/O_2 torch igniter was 1.0–3.0. Here, mass flow rate of the main flow including H_2 fuel was 1750 g/s for a bulk equivalence ratio of 0.4 and a total temperature of airflow of 1500 K. That of the stoichiometric H_2/O_2 torch igniter was 0.37 g/s, 0.02% of that of the main flow, for a total input energy of 5 kW. A spark plug in the combustion chamber then ignited the H_2/O_2 mixture, and the combustion gas was injected vertically into the airflow under a choked condition. Operating conditions of the H_2/O_2 torch igniter and plasma torch igniters[4] are listed in Table 1.

Table 1 Operating conditions of plasma torch igniters[3,4] and H_2/O_2 torch igniter used in the ignition experiment

Parameter	H_2/O_2 torch igniter	Plasma torch igniter
Feedstock	$H_2 + O_2$	$Air/N_2/O_2/Ar/Ar + H_2$
Cooling	No cooling	Water cooling
Flow rate, Nl/min.	40–285	10–40
Injection orifice diameter, mm	1.4/2.5	1.4/3.2
Total input energy, kW	3.1–37	2.2–5.5

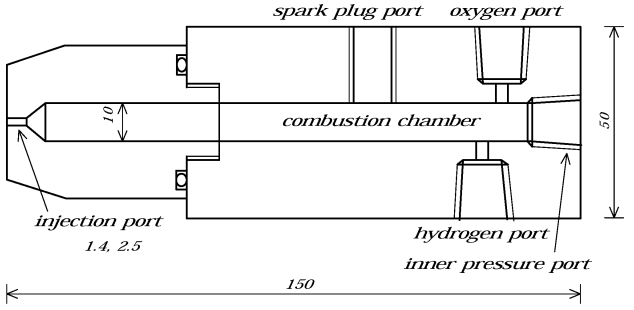

Fig. 11 Schematic diagram of the H_2/O_2 torch igniter for the ignition experiment.

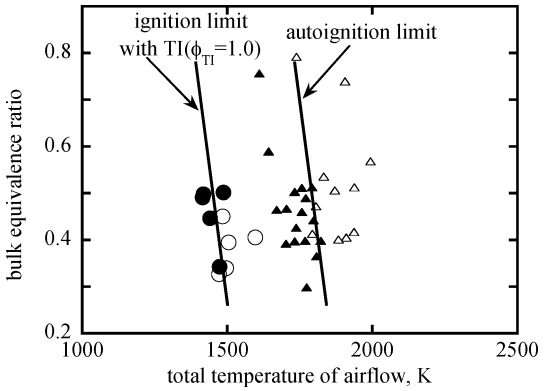

Fig. 12 Effects of the bulk equivalence ratio and a total temperature of airflow on the ignition limit by the H_2/O_2 torch igniter with $E_{total} = 5$ kW.

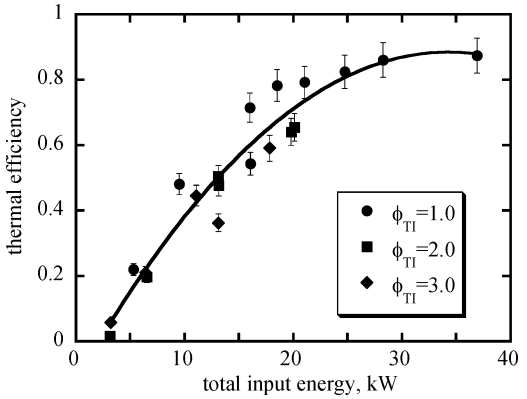

Fig. 13 Thermal efficiency of the H_2/O_2 torch igniter.

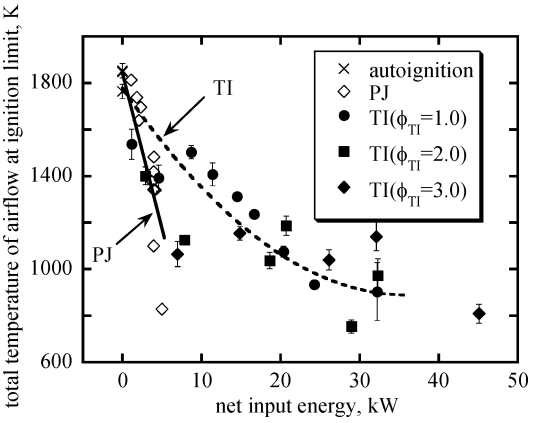

Fig. 14 Effects of net input energy with residual H_2 combustion heat on the ignition limit for $\phi = 0.4$.

Ignition Promotion by the H_2/O_2 Torch Igniter

Figure 12 shows the ignition limit by the H_2/O_2 torch igniter with a stoichiometric condition and a total input energy of 5 kW. Open and solid symbols show ignition and no ignition, respectively. The autoignition limit obtained from ignition experiments without the igniter is also shown in the figure.

Wall-temperature rise for 1.5 s after the initiation of fuel injection was measured at six locations downstream of the step in the streamwise direction. Ignition at each measured point, namely, local ignition, was defined as that when the wall-temperature rise was more than 100 K (Ref. 4). Distribution of the local ignition changed with an increase in airflow total temperature as follows: 1) No local ignition occurred at all of the measured points, 2) local ignition occurred only close to the step, 3) local ignition occurred close to the step and the downstream section of the combustor, and 4) local ignition occurred at all of the measured points.

In the present experiment, ignition limit temperature was defined as the total temperature of airflow at the boundary between 2) and 3). The figure shows that the total temperature of airflow at the autoignition limit for a bulk equivalence ratio of 0.4 is 1800 K and that at the ignition limit by the H_2/O_2 torch igniter is 1500 K at the same bulk equivalence ratio. In other words, the H_2/O_2 torch igniter reduced the ignition limit temperature by 300 K.

Effects of Input Energy on Ignition Promotion

The relationship between net input energy to the igniters and the ignition promotion effect is examined in this section. Net input energy was calculated from the total input energy and thermal efficiency of the igniters. In the case of a plasma torch igniter, the total input energy was given as electric power, and the thermal efficiency was as obtained by Sakuranaka et al.,[19] namely, 70–80% for an N_2 or O_2 plasma. In the case of the H_2/O_2 torch igniter, on the other hand, total input energy was given as the combustion heat of H_2, and the thermal efficiency η_{th} was defined as the function of temperature as follows:

$$\eta_{th} = \frac{c_p \Delta T}{c_p \Delta T_{ad}} = \frac{T_{TI} - 300}{T_{TI,ad} - 300} \tag{18}$$

where T_{TI} is the temperature of combustion gas in the H_2/O_2 torch igniter, and the value of 300 K is the initial temperature of supplied H_2 and O_2, namely, room temperature. Note that enthalpy is linear with temperature under the temperature range observed in the experiment.

The temperature that the gas actually reaches T_{TI} was estimated from mass conservation between input H_2 and O_2 and output combustion gas. The mass flow rate was a function of the discharge coefficient of the orifice through which the jet issues into the combustor flow c_{d_TI}, injection pressure, injection orifice diameter, gas temperature, and molecular weight. The mass flow rates of H_2 and O_2 were determined as already mentioned. For combustion gas, on the other hand, c_{d_TI} and T_{TI} were unknown. Molecular weight of the combustion gas was given as a function of the equivalence ratio in the H_2/O_2 torch igniter. Assuming c_{d_TI} to be 0.90–0.95 yielded T_{TI} with uncertainty. For the H_2/O_2 torch igniter with $\dot{m}_{H_2} = 0.3$ g/s and $\dot{m}_{O_2} = 1.2$ g/s ($\phi_{TI} = 2.0$) and an injection orifice diameter of 2.5 mm, for example, measured P_{TI} was 720 ± 30 kPa. Thus, T_{TI} was obtained as 2120 ± 70 K for $c_{d\_TI} = 0.90$ and 2360 ± 80 K for $c_{d\_TI} = 0.95$. $T_{TI,ad}$ and $P_{TI,ad}$ that the gas would reach if 100% of O_2 reacted with H_2 for the adiabatic condition were evaluated based on two relations, namely, mass conservation and equilibrium condition.

Figure 13 shows the obtained thermal efficiency of the H_2/O_2 torch igniter. The error bars in the figure result from uncertainties in the discharge coefficient of the orifice, which is assumed to lie in the range 0.90–0.95. Thermal efficiency increases with the total input energy because the increment of heat conduction to the igniter is smaller than that of input energy. When the total input energy increases from 10 to 20 kW, for example, thermal efficiency of the H_2/O_2 torch igniter also increases from 40 to 60%.

Figure 14 shows the relationship between net input energy to the igniters and the total temperature of airflow at the ignition limit for a bulk equivalence ratio of 0.4. Results of the plasma torch igniters with open symbols and those of the H_2/O_2 torch igniter for $\phi_{TI} = 1.0, 2.0, 3.0$ with solid symbols are shown in the figure. Masuya et al.[8] showed that the ignition limit of an $H_2 + N_2$ plasma torch igniter was well correlated with the sum of the combustion heat of H_2 in the feedstock and the electric energy input. Therefore, the combustion heat of the residual H_2 of the fuel-rich H_2/O_2 torch igniter and that of H_2 from the $Ar + H_2$ plasma torch igniter were included in the total input energy. The vertical error bars indicate the difference between the maximum temperature with no ignition and the minimum temperature with ignition. For the H_2/O_2 torch igniter, the input energy was controlled by changing the flow rate, so that injection pressure was varied in a wider range than that for the plasma torch igniter. The variation of injection pressure might change a flowfield that determines effective input energy. Therefore, the horizontal error bars are expected to be large for the H_2/O_2 torch igniter.

The ignition limit temperature decreases as input energy to the igniter increases, the reason being that the increase in input energy induces increases in temperature and radical concentration in the igniter injectant. For instance, an increase in input energy from 10 to 20 kW leads to a decrease in ignition limit temperature from 1400 to 1100 K for the H_2/O_2 torch igniter. As expected from the analysis, the figure shows that the H_2/O_2 torch igniter promotes ignition to a lesser degree than does the plasma torch igniter at a given input energy. However, the H_2/O_2 torch igniter has merits of having a lighter battery and a simpler structure than the plasma torch igniter and of having no erosive electrodes. Furthermore, it is easy to increase input energy to the H_2/O_2 torch igniter. To increase total input energy from 5 to 15 kW for the stoichiometric H_2/O_2 torch igniter, for example, the mass flow rate must be increased from 0.37 to 1.1 g/s, which corresponds to only 0.06% of that of main flow including H_2 fuel for a total temperature of 1500 K and an bulk equivalence ratio of 0.4. Therefore, sufficient promotion of ignition can be obtained not only by the plasma torch igniter but also by the H_2/O_2 torch igniter.

There was no significant difference in the promotion of ignition between the stoichiometric H_2/O_2 torch igniter and the fuel-rich one. This shows that the residual hot H_2 is burnt in the airflow and supplies excess radicals and heat to the region of ignition in the combustor. Therefore, the residual hot H_2 from the H_2/O_2 torch igniter contributes to the promotion of ignition. This result shows that required mass flow rate of the H_2/O_2 torch igniter can be decreased to obtain the same input energy. For a total input energy of 15 kW, for instance, an increase of equivalence ratio from 1.0 to 3.0 leads to a decrease of mass flow rate from 1.1 to 0.45 g/s.

Furthermore, a higher equivalence ratio leads to a lower adiabatic temperature for the fuel-rich H_2/O_2 torch igniter. The lower the adiabatic temperature in the H_2/O_2 torch igniter becomes, the less is the thermal load to the spark plug and the injection throat in the igniter without a decrease in the total effect of ignition promotion. Therefore, the fuel-rich H_2/O_2 torch igniter is concluded to be a favorable igniter for the scramjet engine.

Conclusions

The effectiveness of an H_2/O_2 torch igniter, which injects H_2/O_2 combustion gas, and a plasma torch igniter on ignition promotion was investigated analytically and experimentally. The results are summarized as follows:

1) Bulk temperature and bulk radical mole fraction in the O_2 plasma torch igniter with a distributed temperature were estimated by asymptotic analysis to be 1910 K and 0.392, respectively, for an input energy of 140 kJ/mol. Those in the H_2/O_2 torch igniter with a uniform temperature, on the other hand, were also obtained by equilibrium calculation as 3080 K and 0.217 for the same input energy.

2) Gas sampling was conducted to determine the composition of the mixture in the region of ignition, namely, the recirculation region at the base of a rearward-facing step. The mole fraction of the igniter injectant and the local equivalence ratio downstream of the igniter were 10% and 1.0, respectively, for a bulk equivalence ratio of 0.4.

3) Analytical estimation of ignition time of the mixture in the region of ignition with igniters showed that the promotion of ignition by a plasma torch igniter was higher than that of the H_2/O_2 torch igniter at a given input energy. However, it is expected that sufficient promotion of ignition can be obtained not only by the plasma torch igniter but also by the H_2/O_2 torch igniter because it is easy to increase the input energy to the H_2/O_2 torch igniter by increasing the flow rate.

4) Experimental results in Mach 2.5 airflow showed that the H_2/O_2 torch igniter sufficiently promoted ignition as expected from the analysis. Especially, the fuel-rich H_2/O_2 torch igniter, in which residual H_2 contributed to the promotion of ignition and lower flame temperature was obtained, was concluded to be more effective than the stoichiometric one from the viewpoint of mass flow rate and thermal load.

Acknowledgments

Authors wish to thank K. Kudo and A. Murakami, senior researchers in the Combined Propulsion Research Unit, Kakuda Space Propulsion Center, for their assistance in the ignition experiment.

References

[1]Weinberg, F. J., Hom, K., Oppenheim, A. K., and Teichman, K., "Ignition by Plasma Jet," *Nature*, Vol. 272, March 1978, pp. 341–343.

[2]Kimura, I., Aoki, H., and Kato, M., "The Use of a Plasma Jet for Flame Stabilization and Promotion of Combustion in Supersonic Air Flows," *Combustion and Flame*, Vol. 42, 1981, pp. 297–305.

[3]Sato, Y., Sayama, M., Ohwaki, K., Masuya, G., Komuro, T., Kudo, K., Murakami, A., Tani, K., Wakamatsu, Y., Kanda, T., Chinzei, N., and Kimura, I., "Effectiveness of Plasma Torches for Ignition and Flameholding in Scramjet," *Journal of Propulsion and Power*, Vol. 8, No. 4, 1992, pp. 883–889.

[4]Masuya, G., Kudo, K., Murakami, A., Komuro, T., Tani, K., Kanda, T., Wakamatsu, Y., Chinzei, N., Sayama, M., Ohwaki, K., and Kimura, I., "Some Governing Parameters of Plasma Torch Igniter/Flameholder in a Scramjet Combustor," *Journal of Propulsion and Power*, Vol. 9, No. 2, 1993, pp. 176–181.

[5]Northam, G. B., McClinton, C. R., Wagner, T. C., and O'Brien, W. F., "Development and Evaluation of a Plasma Jet Flameholder for Scramjets," AIAA Paper 84-1408, June 1984.

[6]Wagner, T. C., O'Brien, W. F., Northam, G. B., and Eggers, J. M., "Plasma Torch Igniter for Scramjets," *Journal of Propulsion and Power*, Vol. 5, No. 5, 1989, pp. 548–554.

[7]Takita, K., Uemoto, T., Sato, T., Ju, Y., Masuya, G., and Ohwaki, K., "Ignition Characteristics of Plasma Torch for Hydrogen Jet in an Airstream," *Journal of Propulsion and Power*, Vol. 16, No. 2, 2000, pp. 227–233.

[8]Masuya, G., Takita, K., Takahashi, K., Takatori, F., and Ohzeki, H., "Effects of Airstream Mach number on H_2/N_2 Plasma Igniter," *Journal of Propulsion and Power*, Vol. 18, No. 3, 2002, pp. 679–685.

[9]Rogers, R. C., Capriotti, D. P., and Guy, R. W., "Experimental Supersonic Combustion Research at NASA Langley," AIAA Paper 98-2506, June 1998.

[10]Kobayashi, K., Mitani, T., and Niioka, T., "Effects of a Plasma Jet on Ignition in a Supersonic Airflow (in Japanese)," *Proceedings of the Thirty-Fifth Symposium on Combustion*, Combustion Society of Japan, Osaka, 1997, pp. 546–548.

[11]Lochte-Holtgreven, W., *Plasma Diagnostics*, North-Holland, Amsterdam, 1968, pp. 885, 886.

[12]Sudano, J. P., "Nonequilibrium Arc Modeling," *AIAA Journal*, Vol. 22, No. 1, 1984, pp. 148–150.

[13]Chase, M. W., Jr., Davies, C. A., Downey, J. R., Jr., Frurip, D. J., McDonald, R. A., and Syverud, A. N., "JANAF Thermochemical Tables Third Edition," *Journal of Physical and Chemical Reference Data*, Vol. 14, 1985.

[14]Radhakrishnan, K., "LSENS—A General Chemical Kinetics and Sensitivity Analysis Code for Homogeneous Gas-Phase Reactions," NASA RP-1328, 1994.

[15]Mitani, T., Hiraiwa, T., Sato, S., Tomioka, S., Kanda, T., and Tani, K., "Comparison of Scramjet Engine Performance in Mach 6 Vitiated and Storage-Heated Air," *Journal of Propulsion and Power*, Vol. 13, No. 5, 1997, pp. 635–642.

[16]Peters, N., and Williams, F. A., "The Asymptotic Structure of Stoichiometric Methane-Air Flames," *Combustion and Flame*, Vol. 68, 1987, pp. 185–207.

[17]Thayer, W. J., III, and Corlett, R. C., "Gas Dynamic and Transport Phenomena in the Two-Dimensional Jet Interaction Flowfield," *AIAA Journal*, Vol. 10, No. 4, 1972, pp. 488–493.

[18]Zamma, Y., Shiba, H., Masuya, G., Tomioka, S., Hiraiwa, T., and Mitani, T., "Similarity Parameters of Pre-Ignition Flowfields in a Supersonic Combustor," AIAA Paper 97-2890, July 1997.

[19]Sakuranaka, N., Mitani, T., Izumikawa, M., Sayama, M., and Ohwaki, K., "Thermal Efficiency of a Plasma Jet Igniter (in Japanese)," *Proceedings of the Thirty-Third Space Science and Technology Conference*, The Japan Society for Aeronautical and Space Sciences, Tokyo, 1989, pp. 56, 57.